Prolific shedding of magnetite nanoparticles from banknote surfaces

Barbara A. Maher, Tomasz Gonet*

Centre for Environmental Magnetism & Palaeomagnetism, Lancaster Environment Centre, Lancaster University, Lancaster LA1 4YQ, United Kingdom

*Corresponding author: Tomasz Gonet, Centre for Environmental Magnetism and Palaeomagnetism, Lancaster Environment Centre, Lancaster University, LA1 4YQ, UK. E-mail: t.gonet@lancaster.ac.uk.

ABSTRACT

Here, we use magnetic methods first to quantify the content of strongly magnetic particles of banknotes (US dollars, USD, and British pounds sterling, GBP), and then examine the possibility of their release from handled banknote surfaces. The content of magnetic particles, from magnetic remanence measurements, for the USD and paper GBP banknotes is high; greater, for example, than that in vehicle engine-exhaust emissions, and similar to that for airborne roadside particulate matter (PM). Our magnetic analyses of USD and GBP banknotes, and of the ink pigment widely used in their printing, reveal not only that the banknotes are highly magnetic, but also that strongly magnetic, nano-sized particles are readily and prolifically shed from their surfaces (especially from the USD banknotes). A common practice, prior to increased automation, was for bank tellers to count banknotes by licking a finger to adhere to each successive counted note, and thus speed up the manual counting process. Given the rate of particle shedding reported here, this traditional manual counting procedure must have resulted in prolific transfer of iron-rich nanoparticles both to the fingers and thence to the tongue. We hypothesise that, pre-automation, magnetite and other metal-bearing nanoparticles were repetitively and frequently ingested by bank tellers, and subsequently entered the brain directly via the taste nerve pathway, and/or indirectly via the systemic circulation and the neuroenteric system. This hypothesis may plausibly account for the reported and currently unexplained association between elevated neurodegeneration-related mortality odds ratios and this specific occupation.

KEYWORDS: Alzheimer's disease; bank tellers, banknotes, entry portals, Fenton reaction, magnetite, metal-rich nanoparticles, neurodegeneration, Alzheimer's disease

35 Graphical abstract

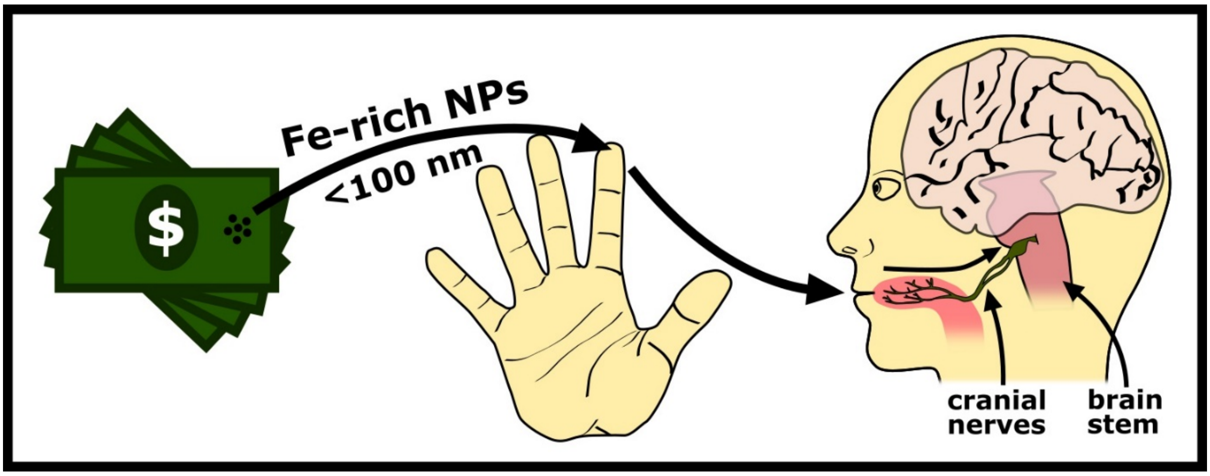

LIST OF ABBREVIATIONS:

AD – Alzheimer's disease
AF – alternating field
ARM – anhysteretic remanent magnetisation
CNS – central nervous system
DC – direct current
GBP – British pound sterling
MDF_{ARM} – median destructive field of ARM
MND – motor neuron disease
MOR – mortality odds ratio
NDD – neurodegenerative disease
PAH – polycyclic aromatic hydrocarbon
PD – Parkinson's disease
PM – particulate matter
PSD – pre-senile dementia
ROS – reactive oxygen species
SIRM – saturation isothermal remanent magnetisation or magnetic remanence
TEM – transmission electron microscopy
USD – United States dollar
X_{ARM} – susceptibility of anhysteretic remanent magnetisation

1. Introduction

The global burden of neurodegenerative disease (NDD) continues to rise, with ~44 million individuals living with dementia (in 2016) and age-standardised incidence increasing from ~701 cases per 100,000 population in 1990 to 712 cases/100,000 population in 2016 (Nichols et al., 2019). Alzheimer's disease (AD) comprises the most prevalent NDD, accounting for 60 – 70% of NDD cases (WHO, 2019). Given the irreparable neuronal damage already incurred once dementia symptoms are manifest, prospects for post-onset therapeutic intervention and disease modification appear very limited. As dementia has severe, negative impacts on individuals, communities and health care systems, increased understanding of risk factors – and subsequent identification of potential pathways to prevention – thus become ever more important.

In comparison with studies of genetic and lifestyle factors, relatively little attention has so far been focused on potential NDD risk factors associated with an individual's occupation (Costa & Manzo, 1998). It is likely that occupational exposures to a range of potential neurotoxicants (Doty, 2008; Costa *et al*., 2014; Pelclova et al., 2016) might provide multiple routes to the common features of neuronal damage associated with NDD, including oxidative stress, protein misfolding and abnormal calcium signalling (Park et al., 2005).

Schulte et al. (1996) examined mortality data, from 1982 to 1991, in 27 U.S.A. states, and identified occupations with elevated mortality rates for AD, Parkinson's disease (PD), motor neuron disease (MND), and pre-senile dementia (PSD). In a follow-up, case-control study, Park et al. (2005) examined mortality and occupational data for deaths attributed or including reference to AD, PD, MND and PSD, for 22 participating U.S.A. states, for the period 1992 – 1998. In addition to testing the occupation/NDD associations identified in the original Schulte et al. (1996) study, Park et al. (2005) assessed hypothesized occupational exposure associations for solvents, magnetic fields, pesticides, and welding (Levy & Nassetta, 2003). For AD, the largest increases in mortality odds ratios (MORs) were associated with an apparently diverse range of occupations, including bank tellers, clergy, aircraft mechanics and hairdressers. For PSD, increased MORs were associated with dentists, clergy and graders/sorters (non-agricultural); for MND, veterinarians, hairdressers, and graders/sorters; for PD, teachers, biological scientists, and clergy. Farmers < 65 yrs in age displayed elevated

MORs for PD, AD and PSD. Occupational exposure to 60 Hz magnetic fields displayed an exposure-response for AD, and for those < 65 yrs, for PD and MND. Welding was associated with PD in those < 65 yrs in age at death.

Exposure to specific physical and chemical agents known to produce oxidative stress has been inferred to account for many of these observed associations between occupation and elevated MORs for NDD. For example, dentists have been exposed to mercury; farmers to organophosphate-rich pesticides; hairdressers to a range of solvents and often metal-bearing dyes; mechanics to engine emissions; welders to manganese. One occupational group reported by Park et al. (2005) to display significantly elevated MORs for AD (MOR = 1.40; 95% CI = 1.14 – 1.70; p = 0.001), yet arguably with no obvious route of neurotoxicant exposure, comprises U.S. bank tellers (who died in the interval 1992 – 1998).

With regard to development of AD and other NDDs, excess iron in some regions of the brain may represent a particular neurological threat. Iron overload can catalyse formation of damaging reactive oxygen species (ROS) via the Fenton reaction (Smith et al., 1997). Iron dyshomeostasis has been linked strongly to the pathogenesis of AD and other NDDs (e.g. Dobson, 2004; Zecca et al., 2004; Castellani et al., 2007). Indeed, discrete nanoparticles of magnetite, a strongly magnetic mixed Fe^{2+}/Fe^{3+} iron oxide, have been found directly associated with AD plaques (Collingwood & Dobson, 2006; Quintana et al., 2006; Plascencia-Villa et al., 2016).

It is possible, however, that endogenous sources and/or mishandling of iron by the brain may represent one part of a much wider problem. Exogenous particles of iron-rich, strongly magnetic magnetite and maghemite, co-associated with other 'exotic' (i.e., non-physiological) metal species (e.g. Cr, Pt, Ce, Mn) have recently been discovered in abundance in the frontal cortex (0.2 – 12 μg/g, corresponding to $2.7 \cdot 10^9$ – $160 \cdot 10^9$ particles/g of freeze-dried tissue) and brainstem regions (0.01 – 2.63 μg/g, corresponding to $0.2 \cdot 10^9$ - $33 \cdot 10^9$ particles/g of freeze-dried tissue) of the human brain (Maher et al., 2016; Calderón-Garcidueñas et al., 2020). Precisely-matching, iron-rich nanoparticles occur abundantly in airborne particulate pollution, including that emitted by traffic, arising from brake-wear, particularly, and from exhaust emissions (Maher et al., 2016; Gonet & Maher, 2019; Zhang et al., 2020). It appears that these iron-rich, airborne nanoparticles, prolific in urban airborne particulate matter (PM), can be transported readily into the brain, whether directly by inhalation via the olfactory bulb (Maher et al., 2016), and/or through ingestion/swallowing and transfer via the gut wall and neuroenteric system (Calderón-Garcidueñas et al., 2020), or indirectly by the systemic circulation (Lu et al., 2020). Given the essential requirement for the brain to regulate tightly the location, transport and safe storage of iron (to avoid the risk of uncontrolled ROS formation), chronic intake of exogenous iron-rich nanoparticles into the brain may constitute a previously unrecognised environmental risk factor for disruption of key central nervous system (CNS) processes (Maher, 2019), including mitochondrial function, myelination and neurotransmitter signalling.

It is also possible that this new hypothesis, of a causal link between exposure to iron-rich pollution nanoparticles and development of NDD (Maher et al., 2016; Maher, 2019), might account for several previously unresolved associations between occupation and NDD. Acute or chronic exposure would be predicted for occupations involving frequent and/or prolonged intervals of inhalation and/or ingestion of such iron- and co-associated metal-rich nanoparticles, produced in abundance by a notably diverse range of sources. In the outdoor environment, these sources include: traffic-related air pollution, arising from exhaust emissions and, especially, brake-wear (Gonet & Maher, 2019; Gonet et al., 2021); industrial emissions, especially from power generation plants (Szuszkiewicz et al., 2015) and steelworks (Zajzon et al., 2013); welding (Sowards et al., 2008) and biomass burning (McClean & Kean, 1993). At-risk occupations might therefore include professional drivers, engine mechanics, steelworkers, welders and farmers. In the indoor environment, iron-rich, and strongly magnetic nanoparticles are emitted from, for example, some printer inks (Gminski et al., 2011), metal lathes (Chen et al., 2020), open fires (Maher et al., 2020b), and candles (Halsall et al., 2008). At-risk occupations might thus also include, for example, office workers, and machinists.

Here, given the elevated MORs reported for NDD in US bank tellers (who died between 1992 and 1998; Park et al., 2005), we examine magnetic properties of GBP and USD banknotes and the possibility of shedding of magnetite nanoparticles from the banknotes' surfaces. We use magnetic measurements to quantify the magnetic content of banknotes, and the release of strongly magnetic particles from their surfaces. We also assess the concentration and particle size of magnetic particles in Pigment Black 11 ink. Until very recently, the composition of banknotes has been cellulose-based, frequently coated with kaolinite (for opacity, and printability) and starch (for wet rub resistance). Universally, and over many decades, iron has been used in the black printing inks used in banknote production, in the form of the pigment known as 'Pigment Black 11', or 'Magnetic Black'. Not only do the banknotes display very high contents of ultrafine magnetite (especially the US dollars), they also shed magnetite particles prolifically from their surfaces. Given the elevated, currently unexplained MORs for NDD reported for US bank tellers (who died between 1992 and 1998), we hypothesise that manual counting of banknotes (i.e., prior to automation from ~1980) resulted in exposure to these metal-rich particles through the taste nerve pathway, directly into the CNS, and/or via swallowing and transfer from the gut wall into the neuroenteric system, and/or dermal absorption. Such exposure through the working lifetime of these US bank tellers may constitute a plausible specific mechanism for excess CNS intake of iron-rich and co-associated toxic metals (specifically, lead), and subsequent neurodegeneration. Critically and prospectively, such a hypothesis would also indicate that, at the present day, occupations linked with excess exposure to iron-rich nanoparticles might also be causally linked with neurodegeneration. Further, newly-developing technologies, such as metal 3D printing (Chen et al., 2020), may be creating new versions of this specific occupational exposure and risk.

2. Materials and Methods

To quantify the content and particle size of any magnetic particulates, and how easily such particles might be shed from the surfaces of banknotes, we made measurements of the magnetic remanence of a selection of banknotes. U.S. dollar (USD) and British pound sterling (GBP) banknotes were used. As paper banknotes were recently (2016-2020) replaced by polymer banknotes in the U.K., we measured both paper and polymer GBP notes; 3 banknotes of each type (paper and polymer) and value (£5, £10 and £20). For comparison, we measured circulated USD paper banknotes (3 USD banknotes of each value: $1, $5, $10, $20, $50 and $100).

Additionally, standard multipurpose wet wipes, which are magnetically ‘clean’, were used to assess whether strongly magnetic, iron-rich particles can be easily removed from the banknote surfaces. Each banknote was gently wiped for 45 s (each side). The wipes were magnetically measured before and after the wiping process; the difference was attributed to the magnetic particles removed from a banknote surface merely with wiping. We repeated the wiping experiment 3 times, using the same banknotes and new wet wipes each time.

All samples (the banknotes and pigment) were first dried for 24 h in a room with controlled temperature (20^{o}C) and humidity (50%), and subsequently weighed, with a Mettler AT250 balance (accuracy of 0.00001 g). Each measurement was repeated 3 times. No metal tools were used during the laboratory work, to preclude any potential contamination of the samples.

In order to quantify the concentration of iron-rich particles in banknotes and wipes, magnetic remanence measurements were carried out. We used a Newport electromagnet to impart saturation isothermal remanent magnetisation (SIRM) to all samples at 1 Tesla (T) at room temperature. For the banknotes, an AGICO JR-6 spinner magnetometer (noise level ~$5 \cdot 10^{-11}$ Am^2) was used to measure the magnetic remanence (SIRM). Because of their weaker signal, we used a 2G RAPID cryogenic magnetometer (noise level ~10^{-11} Am^2) to measure the magnetic remanence (SIRM) of the wet wipes before and after they were used to simulate handling of the banknotes. Each measurement was repeated 3 times.

The susceptibility of anhysteretic remanent magnetisation (χ_{ARM}) was also measured both for the USD and GBP banknotes, and for the black ink pigment. This parameter is especially sensitive to the presence of magnetic grains ~30 – 50 nm in diameter (Özdemir & Banerjee, 1982; Maher, 1988). Anhysteretic remanent magnetisation (ARM) was imparted to all samples at 80 milliTesla (mT) in 4 different direct current (DC) biasing fields: 0.06 mT, 0.08 mT, 1.0 mT and 1.2 mT, and subsequently measured with a 2G RAPID cryogenic magnetometer. The susceptibility of ARM (χ_{ARM}) was calculated as the slope of the ARM(DC field) linear function.

The magnetite concentrations of the wet wipes, pre- and post-wiping of the banknotes, were estimated from experimental SIRM values for sized, synthetic magnetite powders (Maher, 1988). We used an SIRM value of 6.7 Am^2/kg (for grains < 200 nm; based on our observed particle size distribution of the ink pigment, see Results below) to estimate the mass of magnetite deposited on the wet wipes. We then estimated the number of magnetite particles on the wet wipes, assuming magnetite density of 5.15 g/cm^3 and grain size of ~60 nm (based on the average particle size of the banknote ink pigment, see Results below).

We made a similar suite of magnetic measurements on Pigment Black 11 (or 'Magnetic Black'; Cl 77499, Duranat), the ink long used internationally for printing banknotes. SIRM at 1 Tesla was imposed at room temperature using the Newport electromagnet and subsequently measured with a Molspin Minispin magnetometer (noise level ~10^{-9} Am^2). The SIRM measurements were conducted at room temperature, and, after cooling the sample with liquid nitrogen, at ~77 K. ARM was imparted using a Molspin demagnetiser with ARM attachment, and subsequently demagnetised in alternating fields (AF) of 5 mT, 10 mT, 15 mT, 20 mT, 50 mT and 100 mT. The ARM was measured using the Molspin Minispin magnetometer. The measurement of ARM after each step of AF-demagnetisation enabled determination of MDF_{ARM} (median destructive field of ARM), i.e. the field required to demagnetise 50% of ARM. This parameter is helpful in determination of magnetite grain size (Maher, 1988).

All magnetic measurements were conducted at the Centre for Environmental Magnetism and Palaeomagnetism, Lancaster University, UK.

The Pigment Black 11 ink was additionally analysed with transmission electron microscopy (TEM). Approximately 50 mg of ink pigment was first dispersed in 10 ml of ethanol. Then, 5 µl droplets of the suspension were placed on 2 TEM grids (holey carbon films on copper support grids), one selected at random and scanned using a FEI Titan3 Themis 300 STEM, operated at 300 kV. Imaging of the ink particles was used to obtain the particle size distribution, by measurement of 100 randomly-selected particles with well-defined crystal edges.

3. Results

Measurements of the USD and GBP paper banknotes revealed them to be strongly magnetic (unsurprisingly, since their magnetic signature is one common way of differentiating genuine from counterfeit banknotes). The highest SIRMs were observed for the USD banknotes, ranging from $35.6\cdot10^{-3}$ Am^2/kg ($5 banknote) to $89.3\cdot10^{-3}$ Am^2/kg ($100 banknote). The paper GBP banknotes had slightly lower values; $35.0\cdot10^{-3}$ Am^2/kg for £10, $28.9\cdot10^{-3}$ Am^2/kg for £20, and $24.6\cdot10^{-3}$ Am^2/kg for the £5 notes. The concentrations of ferromagnetic grains, as measured by SIRM, in the USD and paper GBP banknotes are notably higher than those in the new, polymer-composition GBP notes (Fig. 1; Table 1). SIRMs for the polymer GBP banknotes (circulated) are ~50 – 130 times lower than those for the paper GBP banknotes, reaching values of $0.47\cdot10^{-3}$ Am^2/kg, $0.42\cdot10^{-3}$ Am^2/kg and $0.26\cdot10^{-3}$ Am^2/kg for the £5, £10 and £20 banknotes, respectively (Fig. 1; Table 1). No notable difference was noted between unused and circulated polymer GBP banknotes (~$0.38\cdot10^{-3}$ Am^2/kg, ~$0.49\cdot10^{-3}$ Am^2/kg and ~$0.26\cdot10^{-3}$ Am^2/kg for the unused £5, £10 and £20 banknotes).

To put these magnetic values into environmental context, Figure 2 shows SIRM values for the USD, paper GBP and polymer GBP banknotes compared with those for a range of indoor and outdoor airborne particulate emissions: specifically, from burning fossil fuels (i.e. peat, wood and coal) in residential open fires; vehicle exhaust emissions (both diesel and petrol); roadside dust; and brake wear emissions. The measured SIRM values for the USD ($35.6 \cdot 10^{-3}$ Am^2/kg – $89.3 \cdot 10^{-3}$ Am^2/kg) and paper GBP banknotes ($24.6 \cdot 10^{-3}$ Am^2/kg – $35.0 \cdot 10^{-3}$ Am^2/kg) are greater than those for diesel- (~$8.6 \cdot 10^{-3}$ Am^2/kg) and petrol-engine (~$5.1 \cdot 10^{-3}$ Am^2/kg) exhaust emissions (Gonet et al., 2021), and PM emitted from open fires (~$8.3 \cdot 10^{-3}$ Am^2/kg) (Maher et al., 2020b); and fall within the range of SIRM values for airborne roadside PM (collected on filters) in Lancaster, U.K. ($7 \cdot 10^{-3}$ Am^2/kg – $167 \cdot 10^{-3}$ Am^2/kg) (Halsall et al., 2008; Fig. 2).

We also measured another magnetic parameter, χ_{ARM}, which is sensitive to the presence of single-domain magnetic grains, i.e., of ~30 – 50 nm in diameter (Maher, 1988). The χ_{ARM} values were very high, with the highest obtained for the USD banknotes ($338 \cdot 10^{-8}$ m^3/kg – $922 \cdot 10^{-8}$ m^3/kg), ~1.4 – 5.6 times higher than those for the paper GBP banknotes ($165 \cdot 10^{-8}$ m^3/kg – $243 \cdot 10^{-8}$ m^3/kg). As with the SIRM values, the χ_{ARM} values for the USD and paper GBP banknotes are notably higher than the polymer-based GBP notes ($3.2 \cdot 10^{-8}$ m^3/kg – $5.4 \cdot 10^{-8}$ m^3/kg) (Fig. 1; Table 1).

Again, to put these magnetic values for the paper banknotes into environmental context, in comparison with our χ_{ARM} values for the GBP paper banknotes, similar values have been reported for total roadside dust (~$150 \cdot 10^{-8}$ m^3/kg - $190 \cdot 10^{-8}$ m^3/kg) in Warsaw, Poland (Dytłow et al., 2019), and for moderately-polluted soil (~$60 \cdot 10^{-8}$ m^3/kg – $470 \cdot 10^{-8}$ m^3/kg) in Shanghai (Hu et al., 2007). In highly polluted areas, χ_{ARM} values can sometimes reach even higher levels, up to ~$5200 \cdot 10^{-8}$ m^3/kg for roadside dust (in south India) (Gargiulo et al., 2016) and ~$3000 \cdot 10^{-8}$ m^3/kg for highly-polluted soil (in Shanghai) (Hu et al., 2007).

Table 1. Mass, saturation isothermal remanence magnetisation (SIRM) and susceptibility of anhysteretic remanent magnetisation (χ_{ARM}) for the USD banknotes, and paper and polymer GBP banknotes (3 banknotes of each type and value; average value ± standard deviation).

Banknote	Mass [g]	SIRM [10^{-3} Am^2/kg]	χ_{ARM} [10^{-8} m^3/kg]
United States dollar (USD) banknotes			
\$1	1.035 ± 0.003	85.8 ± 0.6	922 ± 28
\$5	0.974 ± 0.009	35.6 ± 1.3	338 ± 23
\$10	0.976 ± 0.002	54.4 ± 2.3	662 ± 68
\$20	1.016 ± 0.018	79.6 ± 1.5	779 ± 42
\$50	0.993 ± 0.010	68.8 ± 8.5	708 ± 25
\$100	0.978 ± 0.005	89.3 ± 2.3	857 ± 46
British pound sterling (GBP) banknotes			
Paper £5	0.926 ± 0.026	24.6 ± 2.9	165 ± 12
Paper £10	0.943 ± 0.003	35.0 ± 1.1	243 ± 26
Paper £20	1.091 ± 0.025	28.9 ± 5.1	230 ± 36
Polymer £5	0.754 ± 0.003	0.47 ± 0.03	5.4 ± 1.3
Polymer £10	0.824 ± 0.010	0.42 ± 0.05	3.8 ± 1.0
Polymer £20	0.926 ± 0.003	0.26 ± 0.01	3.2 ± 0.3

In order to assess whether magnetic, iron-rich particles can be easily removed from the banknote surfaces (e.g., by handling for counting purposes), we gently wiped the banknote surfaces with a magnetically-'clean' wet wipe. First, we measured the SIRMs of clean wipes, then we wiped each banknote and measured the wipes again (Table 2). The difference (Δ_{SIRM}) was attributed to the SIRM of the particles removed from each banknote with gentle wiping. In all 36 cases, we found that a portion of magnetic, iron-rich particles was readily removed from the banknotes. Δ_{SIRM} is especially high for the USD banknotes, reaching levels up to $12{,}718 \cdot 10^{-10}$ Am^2 in the first round of wiping (Table 2). In the case of the GBP banknotes, Δ_{SIRM} is lower, ranging between $146 \cdot 10^{-10}$ Am^2 and $244 \cdot 10^{-10}$ Am^2 for the paper GBP banknotes, and between $9 \cdot 10^{-10}$ Am^2 and $187 \cdot 10^{-10}$ Am^2 for the polymer GBP notes (Table 2). We repeated the surface wiping test three times, in order to check if the removed magnetic particles merely represented surface dirt, from handling of notes during circulation, and/or any excess, or residual, printing ink post-production. In the second round of wiping, Δ_{SIRM} ranges from $493 \cdot 10^{-10}$ Am^2 to $4{,}927 \cdot 10^{-10}$ Am^2 for USD banknotes, from $50 \cdot 10^{-10}$ Am^2 to $518 \cdot 10^{-10}$ Am^2 for the paper GBP banknotes, and from $27 \cdot 10^{-10}$ Am^2 to $96 \cdot 10^{-10}$ Am^2 for the polymer GBP banknotes (Table 2). In the third round of wiping, Δ_{SIRM} varies between $3{,}054 \cdot 10^{-10}$ Am^2 and $27{,}155 \cdot 10^{-10}$ Am^2 for the USD banknotes, between $16 \cdot 10^{-10}$ Am^2 and $200 \cdot 10^{-10}$ Am^2 for the paper GBP banknotes, and between $35 \cdot 10^{-10}$ Am^2 and $79 \cdot 10^{-10}$ Am^2 for the polymer GBP banknotes (Table 2).

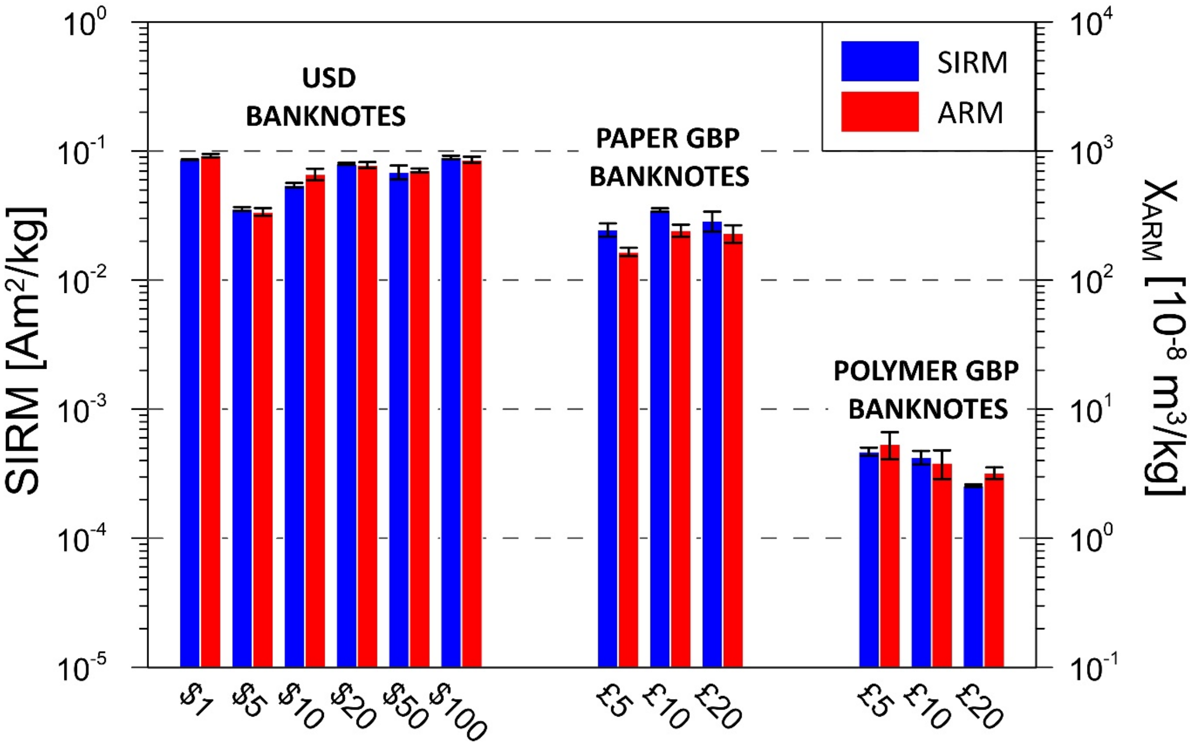

Fig. 1. Saturation isothermal remanent magnetisation (SIRM) and susceptibility of anhysteretic remanent magnetisation (χ_{ARM}) for USD banknotes, and paper and polymer GBP banknotes. Note that the y axis is on a log scale.

Based on SIRMs for sized, pure magnetite powders (Maher, 1988), we can estimate the amount of magnetite removed from the banknotes by each round of gentle wiping. These range from ~45 µg to 190 µg of magnetite being removed, with a single wiping, from the USD banknotes in the first round of wiping (Table 2). Again, in the case of the GBP banknotes, the amount of magnetite easily removable from the banknotes by wiping is much lower, ~2.18 µg to 3.64 µg and ~0.13 µg to 2.79 µg from paper and polymer GBP banknotes, respectively (Table 2). In the second round of wiping, ~7 µg to 74 µg of magnetite is removed from the surface of the USD banknotes, ~0.74 µg to 7.74 µg from the paper GBP banknotes, and ~0.40 µg to 1.44 µg from the polymer GBP banknotes. In the third round of wiping, the mass of the removed magnetite ranges from ~46 µg to 405 µg, ~0.24 µg to 2.99 µg and ~0.52 µg to 1.17

µg for the USD banknotes, paper and polymer GBP banknotes, respectively. The amount of magnetite removed from the banknote surfaces is thus variable but similar for all 3 rounds of wiping, indicating that magnetic (nano)particles shedding from the banknote surfaces originate from the ink pigment, rather than a surface environmental contamination or production-related ink excess.

In order to assess the particle size distribution of the magnetite particles shedding readily from the banknote surfaces, we measured several magnetic parameters for a sample of Pigment Black 11 (Table 3), the pigment traditionally used in printing paper banknotes. We observed extremely high values of room-temperature SIRM (12.6 Am^2/kg) and χ_{ARM} ($212.5 \cdot 10^{-5}$ m^3/kg) (Table 3); indeed, comparable with values for pure magnetite powders (Maher, 1988). Pure magnetite particles which are > 200 nm in diameter usually have χ_{ARM} values < $100 \cdot 10^{-5}$ m^3/kg (Maher, 1988). The χ_{ARM} value obtained for Pigment Black 11 is notably higher ($212.5 \cdot 10^{-5}$ m^3/kg), indicating that it is dominated by magnetite particles < 200 nm. Demagnetisation of the pigment's χ_{ARM} removes half of its initial value by a low demagnetising field, 13 mT, also characteristic of magnetically-'soft', nano-sized magnetite particles (Maher, 1988). We can further narrow down the dominant size of the pigment's magnetite particles by measuring its SIRM at low temperature (77 K). The $SIRM_{77K}$ increases by 28% (15.4 Am^2/kg compared to the $SIRM_{RT}$ value of 12.6 Am^2/kg; Table 3), indicating the presence of 'superparamagnetic' grains (~20-30 nm in size), which are thermally-agitated at room temperature (and thus contribute no magnetic remanence) but which 'block in' at low temperature, contributing the observed $SIRM_{77K}$ increase.

To obtain independent confirmation of the ink particle size, we analysed the ink pigment particles using high-resolution TEM. Its mineralogy confirmed by electron diffraction, the particle size of the magnetite ink ranges between ~15 nm and 400 nm (Fig. 3), with the majority (~80%) being smaller than 100 nm (Fig. 3D).

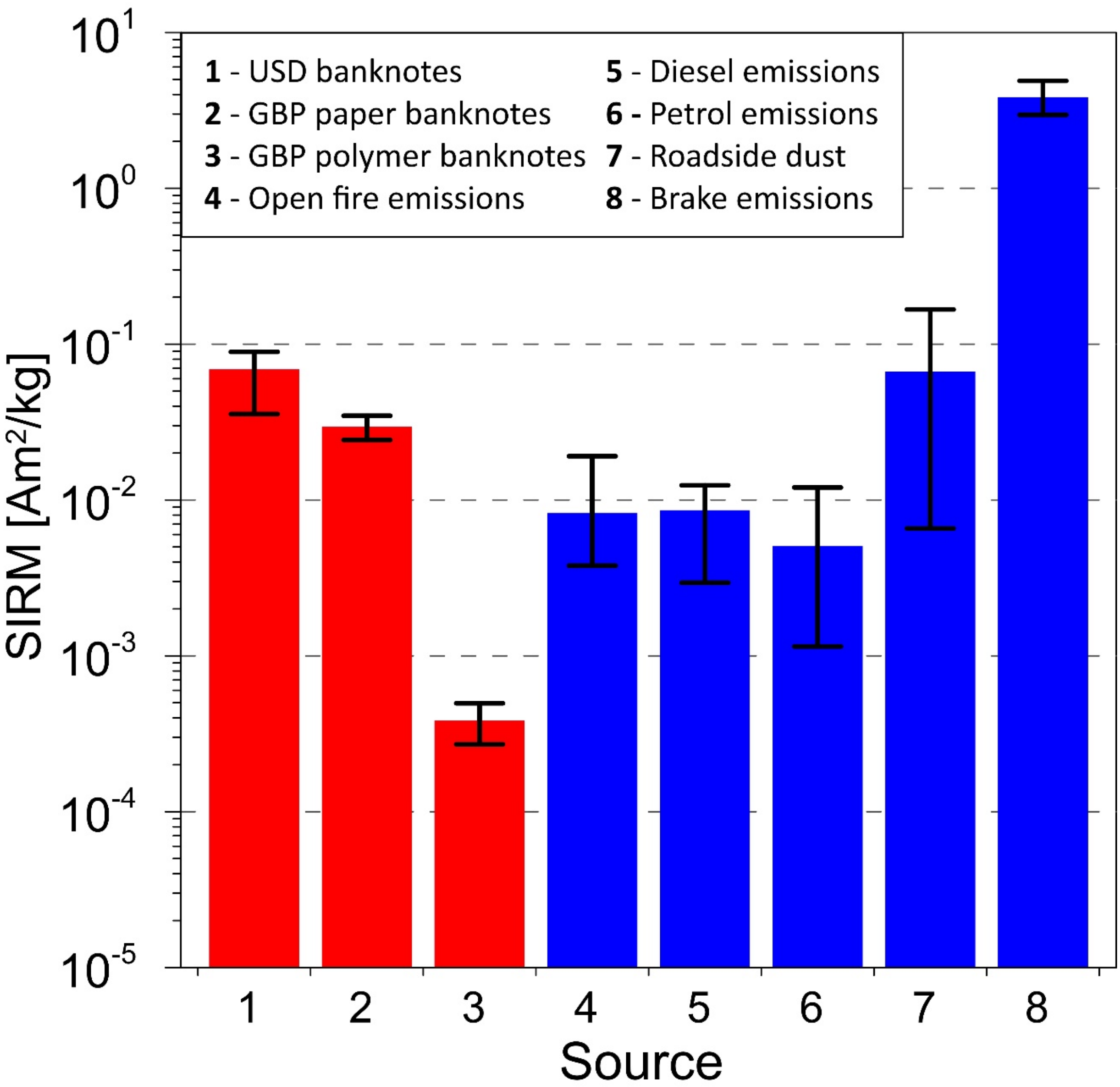

Fig. 2. Saturation isothermal remanent magnetisation (SIRM) for: (1) USD banknotes, (2) paper and (3) polymer GBP banknotes, (4) emissions from open fires (Maher et al., 2020b), (5) vehicle diesel exhaust emissions (Gonet et al., 2021), (6) vehicle petrol exhaust emissions (Gonet et al., 2021), (7) roadside airborne PM (Halsall et al., 2008) and (8) brake-wear PM (Gonet & Maher, 2019). Note the y axis is shown on a log scale.

4. Discussion

It is critical to understand the processes and exposure pathways through which certain occupational groups appear to have become unusually susceptible to development of neurodegenerative disease. Although it has been established that some occupational groups experience(d) exposures to known neurotoxicants, other groups also display significant elevation in neurodegeneration-linked MORs yet have no known or obvious disease aetiology (Schulte et al., 1996; Park et al., 2005). From a study of death certificate information for 22 contributing U.S. states for the interval 1992 – 1998, bank tellers were reported to display elevated – and unexplained – MORs for both pre-senile dementia and Alzheimer’s disease (Park et al., 2005). Given that iron overload and cell damage through excess oxidative stress have been implicated increasingly in neurodegenerative disease (e.g. Quintana et al., 2006; Castellani et al., 2007; Smith et al., 2010; Tabner et al., 2011), it seems timely and important to assess possible routes of metal-rich neurotoxicant exposure in this particular, currently enigmatic occupational group.

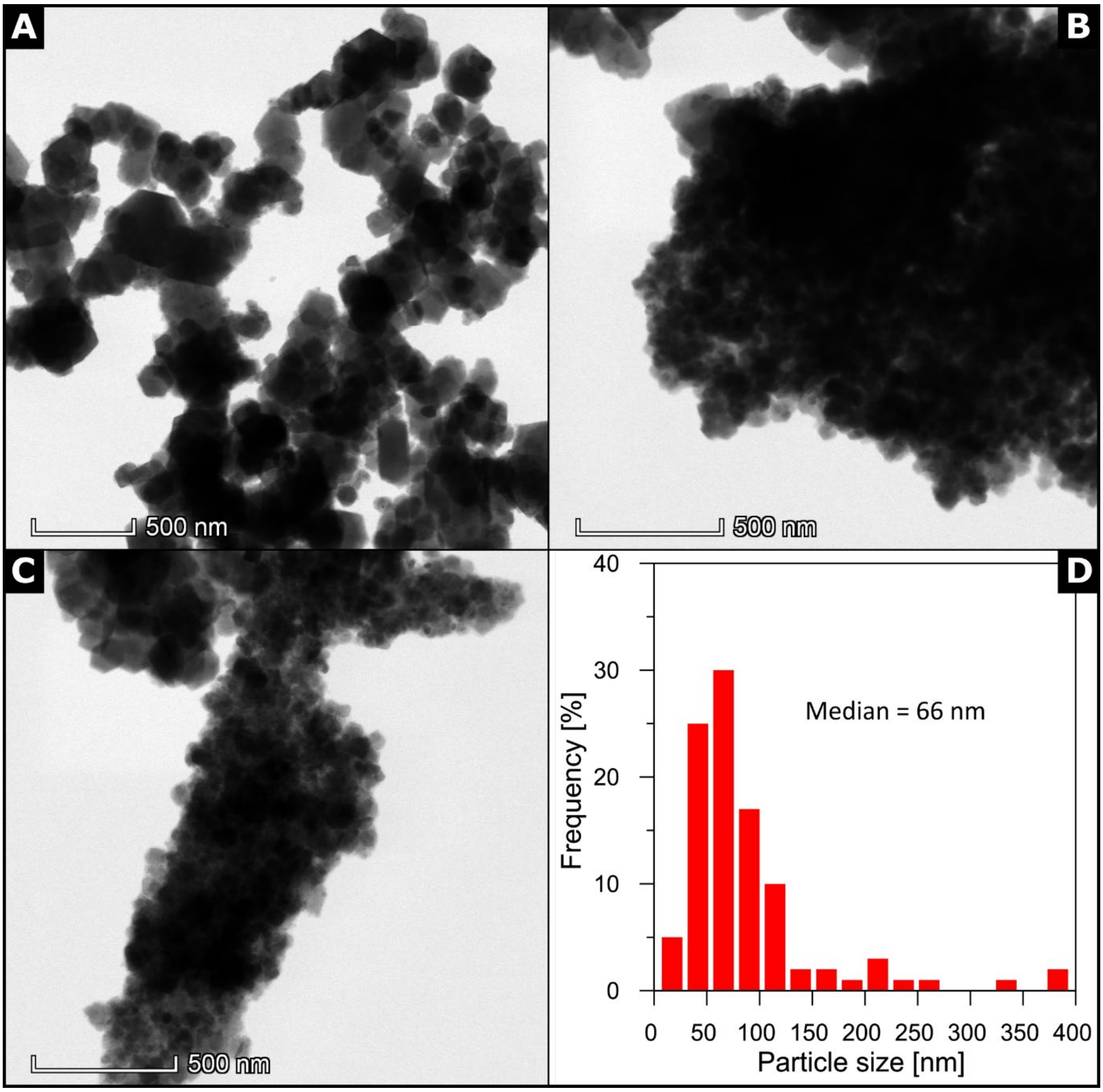

Fig. 3. TEM images of Pigment Black 11 particles (A, B and C) and their particle size distribution (D).

Our approach builds upon the growing body of work which demonstrates that exposure to urban airborne PM is associated not only with respiratory and cardiovascular problems, but also neurodegeneration and cognitive impairments (Calderón-Garcidueñas *et al*., 2002; Pope & Dockery, 2006; Hoek *et al*., 2013; Beelen *et al*., 2014; Costa *et al*., 2014;

Weichenthal *et al*., 2017; Liu *et al*., 2018; Malik *et al*., 2019; Maher *et al*., 2020a). Both indoor and outdoor PM often comprises a complex mixture of components, some of which might be toxic (e.g. Karlsson et al., 2006; Jordanova et al., 2012; Yang et al., 2016; Maher, 2019). Iron-rich and often strongly magnetic nanoparticles are particularly abundant in the solid (non-volatile) fraction of ultrafine (< 100 nm in diameter) air pollution. Because iron can catalyse the formation of reactive oxygen species (ROS), inducing oxidative stress, such iron-rich nanoparticles (whether or not dissolved in the brain subsequently) might constitute a specific neurotoxicant, potentially contributing to the oxidative stress and Alzheimer-like pathology in the human brain (Maher, 2019). Importantly, not only can iron-rich nanoparticles be toxic on their own; they are also often co-associated with other toxic metals, including Al, Ce, Cr, Co, Cu, Mn, Ni, Pb, Pt, Ti and Zn (Spassov et al., 2004; Chen et al., 2006; Kim et al., 2007; Maher et al., 2016, Yang et al., 2016, Hofman et al., 2020) and surface-adsorbed organic species, including polycyclic aromatic hydrocarbons (PAHs) (Lehndorff & Schwark, 2004, Halsall et al., 2008).

Iron-rich nanoparticles, with characteristic high-temperature (> 100°C) surface features and shapes, co-associated with other exogenous metal species, have been found in cortical and brainstem samples in the brains even of young people (< 35 yrs old) exposed lifelong to high concentrations of airborne PM (Maher et al., 2016; Calderón-Garcidueñas et al., 2020). Compared to low-pollution controls, who demonstrate little neuropathology and up to 10 x lower brain nanoparticle numbers, these highly-exposed young people already display multiple aberrant proteinopathies (Calderón-Garcidueñas et al., 2020). Such associations between exposure to airborne, metal-rich pollution particles (dominated by iron-bearing compounds), the abundant presence of precisely-matching nanoparticles inside both autonomous and cortical brain regions, and substantial neuropathologies even in young people, strongly indicates a causal neurodegenerative role for inhaled and ingested metal-rich air pollution nanoparticles (Maher et al., 2016; Calderon-Garciduenas et al., 2020).

Table 2. Saturation isothermal remanent magnetisation (SIRM) for wipes before and after wiping banknote surfaces (3 banknotes of each type and value; average value ± standard deviation).

Banknote that was wiped		SIRM for wipes [10^{-10} Am^2]			Magnetite removed from the banknote [μg]
		Before wiping	After wiping	Difference (Δ_{SIRM})	
1st wiping					
USD banknotes	$1	73 ± 1	10,989 ± 2,145	10,916 ± 2,146	163 ± 32
	$5	72 ± 4	3,109 ± 1,188	3,037 ± 1,183	45 ± 18
	$10	73 ± 2	4,142 ± 763	4,070 ± 761	61 ± 11
	$20	65 ± 7	12,783 ± 3,620	12,718 ± 3,627	190 ± 54
	$50	61 ± 1	5,837 ± 1,422	5,776 ± 1,423	86 ± 21
	$100	65 ± 4	5,723 ± 1,237	5,659 ± 1,234	84 ± 18
GBP banknotes	Paper £5	69 ± 6	313 ± 125	244 ± 120	3.64 ± 1.79
	Paper £10	109 ± 23	254 ± 63	146 ± 53	2.18 ± 0.79
	Paper £20	73 ± 34	285 ± 127	212 ± 154	3.16 ± 2.30
	Polymer £5	67 ± 3	254 ± 77	187 ± 75	2.79 ± 1.12
	Polymer £10	37 ± 3	166 ± 60	129 ± 57	1.93 ± 0.85
	Polymer £20	55 ± 9	63 ± 3	9 ± 7	0.13 ± 0.10
2nd wiping					
USD banknotes	$1	58 ± 3	2,231 ± 206	2,173 ± 203	32 ± 3
	$5	57 ± 1	550 ± 38	493 ± 39	7 ± 1
	$10	58 ± 1	1,958 ± 441	1,900 ± 441	28 ± 7
	$20	61 ± 2	4,988 ± 400	4,927 ± 398	74 ± 6
	$50	59 ± 1	2,022 ± 669	1,963 ± 669	29 ± 10
	$100	61 ± 6	3,006 ± 305	2,946 ± 299	44 ± 4
GBP banknotes	Paper £5	63 ± 15	210 ± 21	147 ± 19	2.19 ± 0.29
	Paper £10	68 ± 7	118 ± 21	50 ± 26	0.74 ± 0.39
	Paper £20	71 ± 4	589 ± 359	518 ± 361	7.74 ± 5.39
	Polymer £5	60 ± 4	156 ± 15	96 ± 17	1.44 ± 0.26
	Polymer £10	55 ± 4	94 ± 5	40 ± 8	0.59 ± 0.12
	Polymer £20	55 ± 1	81 ± 23	27 ± 22	0.40 ± 0.33
3rd wiping					

USD banknotes	$1	64 ± 4	27,219 ± 785	27,155 ± 781	405 ± 12
	$5	64 ± 1	3,118 ± 578	3,054 ± 578	46 ± 9
	$10	65 ± 3	5,439 ± 861	5,374 ± 864	80 ± 13
	$20	67 ± 5	6,021 ± 1,704	5,954 ± 1,710	89 ± 26
	$50	63 ± 2	8,872 ± 626	8,809 ± 628	131 ± 9
	$100	69 ± 4	9,886 ± 1,262	9,817 ± 1,262	147 ± 19
GBP banknotes	Paper £5	53 ± 1	99 ± 27	46 ± 27	0.69 ± 0.41
	Paper £10	61 ± 15	77 ± 5	16 ± 12	0.24 ± 0.17
	Paper £20	62 ± 17	262 ± 147	200 ± 154	2.99 ± 2.30
	Polymer £5	54 ± 1	133 ± 30	79 ± 31	1.17 ± 0.46
	Polymer £10	53 ± 2	91 ± 14	38 ± 14	0.57 ± 0.20
	Polymer £20	54 ± 1	89 ± 4	35 ± 4	0.52 ± 0.06

Hence, chronic exposures to environmental iron-rich nanoparticles may be an important route into neurodegenerative disease. Here, our magnetic analyses of USD and GBP banknotes, and of the ink pigment widely used in their printing, have revealed not only that the banknotes (especially the USD and paper GBP notes) are highly magnetic, but also that strongly magnetic nano-sized particles are shed readily and repeatedly from their surfaces. Just gentle wiping of the banknote surface by a moist wipe resulted in transfer of very high numbers of magnetite particles ($12 \cdot 10^9$ – $695 \cdot 10^9$ for the USD banknotes; $0.4 \cdot 10^9$ – $13 \cdot 10^9$ for paper and $0.2 \cdot 10^9$ – $4.8 \cdot 10^9$ for polymer GBP banknotes) from the banknote to the wipe. Magnetite particles continued to be shed from all banknote surfaces over three successive wipings.

We hypothesise that such shedding of iron-rich, magnetic nanoparticles may provide a possible insight into the elevated MORs observed for U.S.-based bank tellers who died during the period 1992 – 1998. A common practice, prior to increased automation, was for bank tellers to count banknotes by licking a finger to adhere to each successive counted note, and thus speed up the manual counting process. Given the rate of particle shedding reported here, this traditional manual counting procedure must have resulted in prolific transfer of iron-rich nanoparticles first to the fingers (with the possibility of some dermal absorption) and thence to the tongue. Critically, the tongue is an effective and direct pathway to the brain via the taste nerve translocation pathway (VII and IX cranial nerves); readily demonstrated in animal models by elicitation of CNS neurotoxicity through glossal instillation of metal-bearing (Zn, Ti) nanoparticles (Chen et al., 2017; Liang et al. 2018).

This postulated route to an occupational exposure to a potential neurotoxicant specific to bank tellers (in pre-automation times) is somewhat reminiscent of that of the so-called 'radium girls', in the early 20th century. Female factory workers at three United States Radium factories contracted radiation poisoning from painting watch dials with radioluminescent paint. Having been told that the paint was harmless, they were advised to 'point' their brushes with their tongue or lips, to produce a fine paintbrush tip. As a result of ingestion of this radioactive substance, unknown numbers of the women died, typically having developed anaemia, bone fractures and necrosis of the jaw ('radium jaw') (e.g. Gunderman & Gonda, 2015; Cohen & Kim, 2017).

Table 3. Magnetic parameters for Pigment Black 11 (Cl 77499).

Magnetic parameter	**Value**
SIRM [Am^2/kg]	12.6
$SIRM_{77K}$ [Am^2/kg]	15.4
χ_{ARM} [10^{-5} m^3/kg]	212.5

MDF_{ARM} [mT]	13

* $SIRM_{77K}$ – SIRM measured at 77 K

For the U.S.-based bank tellers who died in the interval 1992 – 1998, and started their working lives from ~1930 onwards (assuming the U.S. average lifespan in the 1990s of 79 yrs for women and 72 yrs for men), glossal exposure not only to magnetite-rich particles but also to other cytotoxic metal-bearing particles is additionally likely. Lead, for example, was used in 'Brunswick Green' ink ($PbSO_4 \cdot xPbCrO_4 \cdot yFe_4[Fe(CN)_6]$) at intervals (1928 – 1963, 1969, 1977 – 1988) before being phased out for health reasons; chromium oxide (Cr_2O_3) replacing lead in 'Pigment Green' (Hall & Chambliss, 2004). Titanium dioxide (TiO_2) has been used in production of U.S. banknotes since 1934, as a paper whitener (presaging the vast international expansion in synthesis and use of TiO_2 for diverse applications, from food additives, to cosmetics, paints, plastics and electronics (e.g. Chen & Mao, 2007)).

Given the human, societal and economic costs of the pandemic of neurodegenerative disease, growing year on year as average lifespans increase around the world, it is increasingly urgent and important to identify the diverse pathways of exposure to metal-rich nanoparticles as plausible and pervasive neurotoxicants. Our analysis and discussion here are focused on the potential exposure experienced, pre-automation, by bank tellers (who died between 1992 and 1998). Prospectively, however, these results also indicate that current and newly-developing occupational routes might be inducing harmful exposures. For instance, operators of 3D metal printers (Chen et al., 2020), might be exposed to harmful levels of iron-rich neurotoxicants. Indeed, the prevalence of iron-rich nanoparticles in the environment may even be growing. Iron-rich and strongly magnetic nanoparticle powders, easily and cheaply produced, are increasingly widely used as pigments, catalysts, fillers and even brake friction materials (i.e. designed to be abraded and consequently efficiently released into roadside air). The abundant and pervasive presence of magnetite nanoparticles in both indoor (Maher *et al*., 2020b) and outdoor (Sanderson *et al*., 2016; Gonet & Maher, 2019) environments indicates growing levels of human exposure to these potentially neurotoxic particles, especially if individuals are exposed not only during daily commuting, but also at home (e.g. when using open fires for heating) and, as hypothesised here, at their place of work.

5. Conclusions

1. Because of the magnetic pigments used in their production, banknotes (especially paper banknotes) are strongly magnetic; equivalent in their magnetite concentrations to, for example, the air pollution particles emitted at heavily-trafficked roadsides.

2. Even gentle wiping of paper banknotes (here, with a moist wipe) results in the ready, abundant and repeated shedding of strongly magnetic particles, even up to $\sim 7 \cdot 10^{11}$ particles per wiping. Such shedding of magnetic particles was observed both for U.S. and British banknotes, but was greatest for the USD.

3. The black pigment, ‘Black 11/Magnetic Black’, used for many decades in the printing of banknotes, consists of almost pure magnetite, characterised by nanoscale particulate dimensions, with the majority smaller than 100 nm. Such particles are sufficiently small to access all major organs of the human body, whether by inhalation, ingestion or the taste nerve pathway, and to enter critical sub-cellular organelles, including mitochondria.

4. Excess iron loading in the brain can catalyse excess formation of reactive oxygen species, inducing oxidative stress and cell damage or death. Given the high content and prolific shedding of magnetite nanoparticles we observe from banknote surfaces, we hypothesise that magnetite and other metal-bearing nanoparticles were repetitively and frequently ingested by bank tellers (pre-automation), and subsequently entered the brain directly via the taste nerve pathway and/or indirectly via the systemic circulation and the neuroenteric system. Such an exposure route may plausibly account for the reported and currently unexplained association between elevated neurodegeneration-related MORs and this specific occupation (in a cohort who died between 1992 and 1998).

5. Notwithstanding that neurodegenerative diseases encompass neuropathological and genetic variants, and potentially differing aetiologies, given the scale and costs of such disease on the international scale, investigation of current and newly-developing occupational groups with high exposure to iron-rich nanoparticles, in terms of incidence of neurodegenerative disease, seems both warranted and timely, in combination with well-controlled prospective studies.

Acknowledgements

The authors thank Zabeada Aslam of Leeds University's EPSRC Nanoscience and Nanotechnology Facility (LENNF), U.K. for her assistance in this work. The authors declare no competing financial interest. T. Gonet is funded by a PhD studentship from Jaguar Land Rover. We appreciate the reviewers' comments, which improved our paper.

References

1. Beelen, R.; Raaschou-Nielsen, O.; Stafoggia, M.; Jovanovic Andersen, Z.; Weinmayr, G.; Hoffmann, B. et al. Effects of long-term exposure to air pollution on natural-cause mortality: an analysis of 22 European cohorts within the multicentre ESCAPE project. *Lancet* **2014**, 383, 785-795.
2. Calderón-Garcidueñas, L.; Azzarelli, B.; Acuna, H.; Garcia, R.; Gambling, T.M.; Osnaya, N.; Monroy, S.; Tizapantzi, M.D.R.; Carson, J.L.; Villareal-Calderon, A.; Rewcastle, B. Air pollution and brain damage. *Toxicologic Pathology* **2002**, 30(3), 373-389.
3. Calderón-Garcidueñas, L.; González-Maciel, A.; Reynoso-Robles, R.; Hammond, J.; Kulesza, R.; Lachmann, I.; Torres-Jardón, R.; Mukherjee, P.S.; Maher, B.A. Quadruple abnormal protein aggregates in brainstem pathology and exogenous metal-rich magnetic nanoparticles. The substantia nigrae is a very early target in young urbanities and the gastrointestinal tract likely a key brainstem portal. *Environmental Research* **2020**, 191, 110139.
4. Castellani, R.J.; Moreira, P.I.; Liu, G.; Dobson, J.; Perry, G.; Smith, M.A.; Zhu, X. Iron: The redox-active center of oxidative stress in Alzheimer disease. *Neurochemical Research* **2007**, 32, 1640-1645.
5. Chen, J.; Zheng, H.; Wang, W.; Liu, H.; Lu, L.; Bao, L.; Ren, L. Resuspension method for road surface dust collection and aerodynamic size distribution characterization. *China Particuology* **2006**, 4(6), 300-303.
6. Chen, X.; Mao, S.S. Titanium dioxide nanomaterials: Synthesis, properties, modifications, and applications. *Chemical Reviews* **2007**, 107, 2891-2959.

7. Chen, A.; Liang, H.; Liu, J.; Ou, L.; Wei, L.; Wu, J.; Lai, X.; Han, X.; Shao, L. Central neurotoxicity induced by the instillation of ZnO and TiO_2 nanoparticles through the taste nerve pathway. *Nanomedicine (Lond)* **2017**, 12(20), 2453-2470.
8. Chen, R.; Yin, H.; Cole, I.S.; Shen, S.; Zhou, X.; Wang, Y.; Tang, S. Exposure, assessment and health hazards of particulate matter in metal additive manufacturing: A review. *Chemosphere* **2020**, 259, 127452.
9. Cohen, D.E.; Kim, R.H. The legacy of the Radium Girls. *JAMA Dermatology* **2017**, 153(8), 801.
10. Collingwood, J.; Dobson, J. Mapping and characterization of iron compounds in Alzheimer's tissue. *Journal of Alzheimer's Disease* **2006**, 10, 215-222.
11. Costa, L.G.; Cole, T.B.; Coburn, J.; Chang, Y.-C.; Dao, K.; Roque, P. Neurotoxicants are in the air: Convergence of human, animal, and *in vitro* studies on the effects of air pollution on the brain. *Hindawi Publishing Corporation* **2014**, 736385.
12. Costa, L.G.; Manzo, L. *Occupational Neurotoxicology*. CRC Press, Boca Raton, Boston, London, New York, Washington, D.C., **1998**.
13. Doty, R.L. The olfactory vector hypothesis of neurodegenerative disease: Is it viable? *Annals of Neurology* **2008**, 63, 7-15.
14. Dytłow, S.; Winkler, A.; Górka-Kostrubiec, B.; Sagnotti, L. Magnetic, geochemical and granulometric properties of street dust from Warsaw (Poland). *Journal of Applied Geophysics* **2019**, 169, 58-73.
15. Gargiulo, J.D.; Kumar, R.S.; Chaparro, M.A.E.; Chaparro, M.A.E.; Natal, M.; Rajkumar, P. Magnetic properties of air suspended particles in thirty eight cities from south India. *Atmospheric Pollution Research* **2016**, 7, 626-637.

16. Gminski, R.; Decker, K.; Heinz, C.; Seidel, A.; Könczöl, M.; Goldenberg, B.; Grobéty, B.; Ebner, W.; Gieré, R.; Mersch-Sundermann, V. Genotoxic effects of three selected black toner powders and their dimethyl sulfoxide extracts in cultured human epithelial A549 lung cells in vitro. *Environmental and Molecular Mutagenesis* **2011**, 52, 296-309.
17. Gonet, T.; Maher, B.A. Airborne, vehicle-derived Fe-bearing nanoparticles in the urban environment: A review. *Environmental Science & Technology* **2019**, 53, 9970-9991.
18. Gonet, T.; Maher, B.A.; Kukutschová, J. Source apportionment of magnetite particles in roadside airborne particulate matter. *Science of the Total Environment* **2021**, 752, 141828.
19. Gunderman, R.B.; Gonda, A.S. Radium Girls. *Radiology* **2015**, 274(2), 314-318.
20. Hall, G.S.; Chambliss, C.R. Nondestructive multi-elemental analyses of current-size United States federal reserve notes by energy dispersive X-ray fluorescence. *Applied Spectroscopy* **2004**, 58(11), 1334-1340.
21. Halsall, C.J.; Maher, B.A.; Karloukovski, V.V.; Shah, P.; Watkins, S.J. A novel approach to investigating indoor-outdoor pollution links: Combined magnetic and PAH measurements. *Atmospheric Environment* **2008**, 42, 8902-8909.
22. Hoek, G.; Krishnan, R.M.; Beelen, R.; Peters, A.; Ostro, B.; Brunekreef, B., Kaufman, J.D. Long-term air pollution exposure and cardio-respiratory mortality: a review. *Environmental Health* **2013**, 12(43).
23. Hofman, J.; Castanheiro, A.; Nuyts, G.; Joosen, S.; Spassov, S.; Blust, R.; De Wael, K.; Lenaerts, S.; Samson, R. Impact of urban street canyon architecture on local atmospheric pollutant levels and magneto-chemical PM_{10} composition: An experimental study in Antwerp, Belgium. *Science of the Total Environment* **2020**, 712, 135534.

24. Hu, X.-F.; Su, Y.; Ye, R.; Li, X.-Q.; Zhang, G.-L. Magnetic properties of the urban soils in Shanghai and their environmental implications. *Catena* **2007**, 70, 428-436.
25. Jordanova, D.; Jordanova, N.; Lanos, P.; Petrov, P.; Tsacheva, T. Magnetism of outdoor and indoor settled dust and its utilization as a tool for revealing the effect of elevated particulate air pollution on cardiovascular mortality. *Geochemistry, Geophysics, Geosystems G^3* **2012**, 13(8).
26. Karlsson, H.L.; Ljungman, A.G.; Lindbom, J.; Möller, L. Comparison of genotoxic and inflammatory effects of particles generated by wood combustion, a road simulator and collected from street and subway. *Toxicology Letters* **2006**, 165, 203-211.
27. Kim, W.; Doh, S.-J.; Park, Y.-H.; Yun, S.-T. Two-year magnetic monitoring in conjunction with geochemical and electron microscopic data of roadside dust in Seoul, Korea. *Atmospheric Environment* **2007**, 41, 7627-7641.
28. Lehndorff, E.; Schwark, L. Biomonitoring of air quality in the Cologne Conurbation using pine needles as a passive sampler – Part II: polycyclic aromatic hydrocarbons (PAH). *Atmospheric Environment* **2004**, 38, 3793-3808.
29. Levy, B.S.; Nassetta, W.J. Neurologic effects of manganese in humans: A review. *International Journal of Occupational and Environmental Health* **2003**, 9, 153-163.
30. Liang, H.; Chen, A.; Lai, X.; Liu, J.; Wu, J.; Kang, Y.; Wang, X.; Shao, L. Neuroinflammation is induced by tongue-instilled ZnO nanoparticles via the Ca^{2+}-dependent NF- κB and MAPK pathways. *Particle and Fibre Toxicology* **2018**, 15(39).
31. Liu, J.-Y.; Hsiao, T.-C.; Lee, K.-Y.; Chuang, H.-C.; Cheng, T.-J.; Chuang, K.-J. Association of ultrafine particles with cardiopulmonary health among adult subjects in the urban areas of northern Taiwan. *Science of the Total Environment* **2018**, 627, 211-215.

32. Lu, D.; Luo, Q.; Chen, R.; Zhuansun, Y.; Jiang, J.; Wang, W.; Yang, X.; Zhang, L.; Liu, X.; Li, F.; Liu, Q.; Jiang, G. Chemical multi-fingerprinting of exogenous ultrafine particles in human serum and pleural effusion. *Nature Communications* **2020**, 11, 2564.
33. Maher, B.A. Magnetic properties of some synthetic sub-micron magnetites. *Geophysical Journal* **1988**, 94, 83-96.
34. Maher, B.A. Airborne magnetite- and iron-rich pollution nanoparticles: Potential neurotoxicants and environmental risk factors for neurodegenerative disease, including Alzheimer's disease. *Journal of Alzheimer's Disease* **2019**, 71(2), 361-375.
35. Maher, B.A.; González-Maciel, A.; Reynoso-Robles, R.; Torres-Jardón, R.; Calderón-Garcidueñas, L. Iron-rich air pollution nanoparticles: An unrecognised environmental risk factor for myocardial mitochondrial dysfunction and cardiac oxidative stress. *Environmental Research* **2020a**, 188, 109816.
36. Maher, B.A.; O'Sullivan, V.; Feeney, J.; Gonet, T.; Kenny, R.A. Indoor particulate air pollution from open fires and the cognitive function of older people. *Environmental Research* **2020b**, 192, 110298.
37. Maher, B.A.; Ahmed, I.A.M.; Karloukovski, V.V.; MacLaren, D.A.; Foulds, P.G.; Allsop, D.; Mann, D.M.A.; Torres-Jardón, R.; Calderón-Garcidueñas, L. Magnetite pollution nanoparticles in the human brain. *Proceedings of the National Academy of Sciences of the United States of America* **2016**, 113(39), 10797-10801.
38. Malik, A.O.; Jones, P.G.; Chan, P.S.; Perl-Okonny, P.; Hejjaji, V.; Spertus, J.A. Association of long-term exposure to particulate matter and ozone with health status and mortality in patients after myocardial infarction. *Circulation: Cardiovascular Quality and Outcomes* **2019**, 12, e005598.

39. McClean, R.G.; Kean, W.F. Contributions of wood ash magnetism to archaeomagnetic properties of fire pits and hearths. *Earth and Planetary Science Letters* **1993** 119, 387-394.

40. Nichols, E.; Szoeke, C.E.I.; Vollset, S.E.; Abbasi, N.; Abd-Allah, F.; Abdela, J.; Taki, M.; Aichour, E., Akinyemi, R.O. et al. (GBD 2016 Dementia Collaborators). Global, regional, and national burden of Alzheimer's disease and other dementias, 1990-2016: a systematic analysis for the Global Burden of Disease Study 2016. *Lancet Neurology* **2019**, 18, 88-106.

41. Özdemir, Ö.; Banerjee, S.K. A preliminary magnetic study of soil samples from west-central Minnesota. *Earth and Planetary Science Letters* **1982**, 59, 393-403.

42. Park, R.M.; Schulte, P.A.; Bowman, J.D.; Walker, J.T.; Bondy, S.C.; Yost, M.G.; Touchstone, J.A.; Dosemeci, M. Potential occupational risks for neurodegenerative diseases. *American Journal of Industrial Medicine* **2005**, 48, 63-77.

43. Pelclova, D.; Zdimal, V.; Kacer, P.; Fenclova, Z.; Vlckova, S.; Syslova, K.; Navratil, T.; Schwarz, J.; Zikova, N.; Barosova, H.; Turci, F.; Komarc, M.; Pelcl, T.; Belacek, J.; Kukutschova, J.; Zakharov, S. Oxidative stress markers are elevated in exhaled breath condensate of workers exposed to nanoparticles during iron oxide pigment production. *Journal of Breath Research* **2016**, 10, 016004.

44. Plascencia-Villa, G.; Ponce, A.; Collingwood, J.F.; Arellano-Jiménez, M.J.; Zhu, X.; Rogers, J.T.; Betancourt, I.; José-Yamacán, M.; Perry, G. High-resolution analytical imaging and electron holography of magnetite particles in amyloid cores of Alzheimer's disease. *Scientific Reports* **2016**, 6, 24873.

45. Pope, C.A.; Dockery, D.W. Health effects of fine particulate air pollution: Lines that connect. *Journal of the Air & Waste Management Association* **2006**, 56, 709-742.

46. Quintana, C.; Bellefqih, S.; Laval, J.Y.; Guerquin-Kern, J.L.; Wu, T.D.; Avila, J.; Ferrer, I.; Arranz, R.; Patiño, C. Study of the localization of iron, ferritin, and hemosiderin in Alzheimer's disease hippocampus by analytical microscopy at the subcellular level. *Journal of Structural Biology* **2006**, 153, 42-54.

47. Sanderson, P.; Su, S.S.; Chang, I.T.H.; Delgado Saborit, J.M.; Kepaptsoglou, D.M.; Weber, R.J.M.; Harrison, R.M. Characterisation of iron-rich atmospheric submicrometre particles in the roadside environment. *Atmospheric Environment* **2016**, 140, 167-175.

48. Schulte, P.A.; Burnett, C.A.; Boeniger, M.F.; Johnson, J. Neurodegenerative diseases: Occupational occurrence and potential risk factors, 1982 through 1991. *American Journal of Public Health* **1996**, 86(9), 1281-1288.

49. Smith, M.A.; Harris, P.L.R.; Sayre, L.M.; Perry, G. Iron accumulation in Alzheimer disease is a source of redox-generated free radicals. *Proceedings of the National Academy of Sciences of the United States of America* **1997**, 94, 9866-9868.

50. Smith, M.A.; Zhu, X.; Tabaton, M.; Liu, G.; McKeel Jr., D.W.; Cohen, M.L.; Wang, X.; Siedlak, S.L.; Hayashi, T.; Nakamura, M.; Nunomura, A.; Perry, G. Increased iron and free radical generation in preclinical Alzheimer disease and mild cognitive impairment. *Journal of Alzheimer's Disease* **2010**, 19(1), 363-372.

51. Sowards, J.W.; Lippold, J.C.; Dickinson, D.W.; Ramirez, A.J. Characterization of welding fume from SMAW electrodes – Part I. Size and mass distributions, fume generation rates, and chemistry are compared for three SMAW electrodes. *Welding Research* **2008**, 87, 106-112.

52. Spassov, S.; Egli, R.; Heller, F.; Nourgaliev, D.K.; Hannam, J. Magnetic quantification of urban pollutant sources in atmospheric particulate matter. *Geophysical Journal International* **2004**, 159, 555-564.
53. Szuszkiewicz, M.; Magiera, T.; Kapička, A.; Petrovský, E.; Grison, H.; Gołuchowska, B. Magnetic characteristics of industrial dust from different sources of emission: A case study of Poland. *Journal of Applied Geophysics* **2015**, 116, 84-92.
54. Tabner, B.J.; Mayes, J.; Allsop, D. Hypothesis: Soluble Aβ oligomers in association with redox-active metal ions are the optimal generators of reactive oxygen species in Alzheimer's disease. *International Journal of Alzheimer's Disease* **2011**, 2011, 546380.
55. Weichenthal, S.; Bai, L.; Hatzopoulou, M.; Van Ryswyk, K.; Kwong, J.C.; Jerrett, M.; Van Donkelaar, A.; Martin, R.V.; Burnett, R.T.; Lu, H.; Chen, H. Long-term exposure to ambient ultrafine particles and respiratory disease incidence in Toronto, Canada: a cohort study. *Environmental Health* **2017**, 16(64).
56. World Health Organization. *Dementia – Fact Sheet*. **2019**. [https://www.who.int/en/news-room/fact-sheets/detail/dementia; accessed April 20th, 2020].
57. Yang, Y.; Vance, M.; Tou, F.; Tiwari, A.; Liu, M.; Hochella Jr., M.F. Nanoparticles in road dust from impervious urban surfaces: distribution, identification, and environmental implications. *Environmental Science: Nano* **2016**, 3, 534-544.
58. Zajzon, N.; Márton, E.; Sipos, P.; Kristály, F.; Németh, T.; Kis-Kovács, V.; Weiszburg, T.G. Integrated mineralogical and magnetic study of magnetic airborne particles from potential pollution sources in industrial-urban environment. *Carpathian Journal of Earth and Environmental Sciences* **2013**, 8(1), 179-186.

59. Zhang, Q.; Lu, D.; Wang, D.; Yang, X.; Zuo, P.; Yang, H.; Fu, Q.; Liu, Q.; Jiang, G. Separation and tracing of anthropogenic magnetite nanoparticles in the urban atmosphere. *Environmental Science and Technology* **2020**, 54, 9274-9284.